Photophysics of Backbone Fluorescent DNA Modifications: Reducing Uncertainties in FRET

Suman Ranjit,[‡,§] Kaushik Gurunathan,[‡,§] and Marcia Levitus*[,§,†,‡]

Department of Chemistry and Biochemistry, Department of Physics and The Biodesign Institute, Arizona State University, Tempe, Arizona 85287-5601

Received: December 9, 2008; Revised Manuscript Received: February 4, 2009

We have investigated the photophysical properties of backbone fluorescent DNA modifications with the goal of reducing many of the sources of uncertainty commonly encountered in Förster resonance energy transfer (FRET) measurements. We show that backbone modifications constrain rotational motions, providing a way by which the orientation of the dye can be controlled in a predictable manner, and reduce the uncertainties in donor−acceptor distance associated with the flexible linkers commonly used in conjugate chemistry. Rotational rigidity also prevents undesirable dye−DNA interactions, which have been shown to affect the photophysical properties of the dye. Unusually large FRET efficiencies for donor−acceptor pairs separated by 102 Å (three helical turns) were measured and attributed to the favorable relative orientation of the dipoles. The same FRET efficiency was measured for a sample in which the donor−acceptor separation was 12 Å shorter, demonstrating the important role of relative orientation in FRET experiments.

Introduction

Förster resonance energy transfer (FRET) is a process in which the excited-state energy of one fluorescent donor molecule is transferred to a neighboring acceptor chromophore in the ground state. The efficiency of transfer depends on the distance between the dyes (R_{DA}), and it can be thus used to measure molecular distances in macromolecules using fluorescent probes bound to specific sites. This technique was pioneered by Stryer, who coined the term "spectroscopic ruler" in 1967.[1] Although FRET measurements have played an important role in the study of the structure and function of nucleic acids for several decades, the popularity of the technique has never been higher thanks to the latest advances in instrumentation and the availability of new and improved fluorescent dyes.[2,3]

According to Förster's theory, the efficiency of FRET (E_{FRET}) depends on the inverse sixth power of the distance between the two dyes:

$$E_{FRET} = [1 + (R_{DA}/R_0)^6]^{-1} \quad (1)$$

The term R_0 is known as the Förster distance and represents the distance at which the efficiency of transfer is 50%. The Förster distance can be calculated as

$$R_o\,(\text{Å}) = [2.8 \times 10^{-5}\kappa^2\phi_D{}^0 J\,]^{1/6} \quad (2)$$

where κ^2 is the orientation factor, $\phi_D{}^0$ is the fluorescence quantum yield of the donor in the absence of FRET, and J represents the spectral overlap of the emission spectrum of the donor with the absorption spectrum of the acceptor normalized on a wavenumber scale.[4]

There are several sources of uncertainty that preclude FRET from being a true quantitative technique, with the orientation factor being the most frequently discussed in the literature.[5−8] Orientation is measured by the famous *kappa square* factor (κ^2), which is determined by the relative orientation between the two dyes and can take values from 0 (perpendicular transition moments) to 4 (collinear transition moments).[5] Since the relative orientation between the two dyes is rarely known, a value of $\kappa^2 = {}^2/_3$ is commonly assumed and used. This value corresponds to the limit in which both the donor and acceptor rotate freely at a rate much faster than the excited-state lifetime of the donor. Historically, flexible linkers have been favored with the purpose of maximizing the rotational freedom of the dye so as to validate the approximation of $\kappa^2 = {}^2/_3$. However, this is seldom true due to the chemical linkage between the dye and the DNA strand.

The carbocyanine Cy3 (Figure 1) is one of the most widely used fluorescent dyes in biophysical research and, in particular, the favorite fluorophore for single-molecule spectroscopy work.[9] It is extensively used by itself or together with Cy5 as the acceptor in FRET measurements. In previous work, we have characterized the photophysical properties of Cy3 covalently attached to DNA through a six-carbon flexible linker[10] and have shown that the dye is neither completely rigid nor does it rotate freely during the lifetime of the excited state. In fact, the flexible linker not only does not guarantee rotational freedom, but it actually allows enough flexibility for the dye to interact with the DNA. Dye−DNA interactions have been reported for a variety of commonly used dyes, including Cy3,[10] Cy5,[11] and the rhodamine dyes Texas Red[12] and tetramethyl rhodamine.[12,13] These interactions not only create an uncertainty in the relative orientations of the donor and acceptor dyes, but also they cause large uncertainties in the donor−acceptor distances. Theoretical simulations have shown that Cy5 bound to dsDNA through a flexible linker binds to the major groove in two distinct conformations, resulting in an average donor−acceptor distance difference of 8 Å between the two conformers.[11] Moreover, it is important to notice that dye−DNA interactions often affect the photophysical properties of the dye, including the fluores-

* Author to whom correspondence should be addressed. E-mail: Marcia.levitus@asu.edu.
§ Department of Chemistry and Biochemistry.
† Department of Physics.
‡ The Biodesign Institute.

10.1021/jp810842u CCC: $40.75
Published on Web 03/26/2009

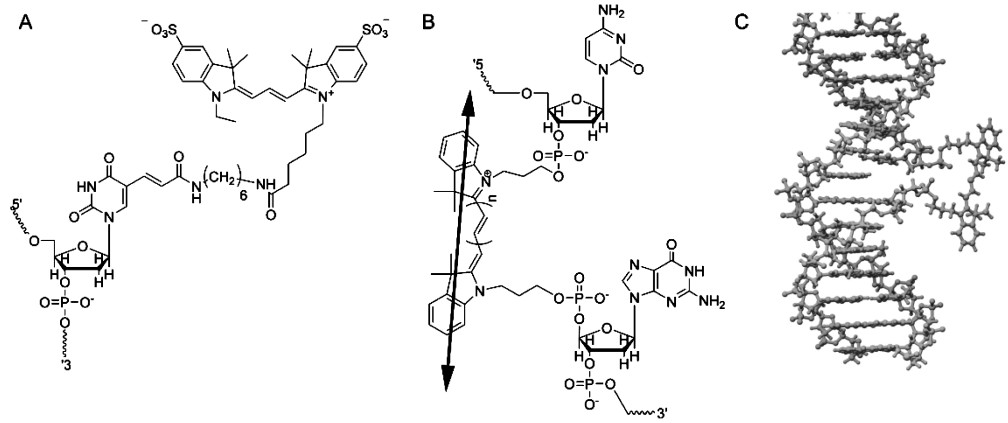

Figure 1. (A) Structure of Cy3 attached to DNA internally through a six-carbon flexible linker. (B) Chemical structure of the *i*Cy3 ($n = 1$) and *i*Cy5 ($n = 2$) backbone modifications used in this work. The arrow represents the orientation of the emission transition dipole moment. (C) The dye replaces one of the bases in the double helix, leaving a base in the complementary strand unpaired.

CHART 1

A: 5'-GATGATGTCATCGAC/iCy3/GCGCGATATTAGCT-3'

B: 5'-CTCTAGCAGGGTAGC/iCy5/CAGGTGCGAGGCTG-3'

C: 5'-GATGATGTCATCGACAGC/iCy3/CGATATTAGCTCTCTAGCAGGGTAGCACAGGTGCGAGGCTG-3'

D: 5'-GATGATGTCATCGAC/iCy3/GCGCGATATTAGCTCTCTAGCAGGGTAGCACAGGTGCGAGGCTG-3'

E: 5'-CAGCCTCGCACCTGTGC/iCy5/ACCCTGCTAGAGAGCTAATATCGCGCTGTCGATGACATCATC-3'

F: 5'-CAGCCTCGCACCTGTGCTACCCTGCTAGAGAGCTAATATCGCGCTGTCGATGACATCATC- 3'

G: 5'-ATGATGTCATCGAC/iAmMC6T/GCGCGATATTAGCTCTCTAGCAGGGTAGCACAGGTGCG AGGCTG-3'

H: 5'-CAGCCTCGCACCTGTGCTACCCTGCTAGAGAGCTAATATCGCGCAGTCGATGACATCATC-3'

cence quantum yield.[10] This introduces further uncertainties in FRET measurements because R_0 depends on the quantum yield of the donor as shown in eq 2.

Here, we investigate a different synthetic approach in which the dye is rigidly attached to the backbone of the DNA (Figure 1B and C). We reasoned that since all of the drawbacks mentioned above are due to the use of flexible linkers, the use of a rigidly attached fluorophore would eliminate most of the uncertainties associated with the method. Our results show that the mobility of these backbone-bound dyes is very limited during the lifetime of the excited state, so the relative orientation of the dyes, as measured by κ^2, remains constant in the time scale relevant for energy transfer. Restricted mobility is also beneficial from the point of view of limiting DNA−fluorophore interactions and reducing the variability in donor−acceptor distance.

Materials and Methods

DNA Samples. The oligonucleotides shown in Chart 1 were purchased from Integrated DNA Technologies (Coralville, IA), where /iAmMC6T/ represents the internal amino modifier C6 dT and /iCy3-5/ represents the backbone Cy3 or Cy5 modification. All strands were HPLC purified, and their mass spectra show a single narrow peak consistent with their predicted molecular weights.

The following samples were prepared using the above oligonucleotides:

Sample 1 was prepared by ligating strands A and B and annealing the product to its complementary sequence (strand F). The ligation step was necessary due to synthetic limitations that prevent the incorporation of both a "*i*Cy3" and a "*i*Cy5" molecule in the same strand with the required distance separation. Ligation was performed following standard procedures. First, strand B was treated with T4 polynucleotide kinase (New England Biolabs, Ipswich, MA), and the product was ligated to strand A using T4 DNA ligase (New England Biolabs, Ipswich, MA) in the presence of strand F, according to the protocol supplied by the manufacturer. The ligated product was purified from a 12% denaturing polyacrylamide gel and annealed to strand F to produce sample 1. Purity was subsequently checked by native electrophoresis.

Samples 2 and 3 were obtained by annealing strands D (sample 2) and C (sample 3) with a complementary strand containing a backbone Cy5 modification (strand E). Purity was subsequently checked by native electrophoresis.

Sample 4 (internally labeled DNA through a six-carbon flexible linker) was prepared from strands G and H. First, strand G was reacted with the monoreactive *N*-hydroxysuccinimidyl (NHS) ester of Cy3, following the recommendations of the supplier (GE Healthcare, Piscataway, NJ). The unreacted dye was removed by size exclusion chromatography using a Micro Bio-Spin *P*6 from Bio-Rad (Hercules, CA), and the purity of the product was checked by gel electrophoresis. The fluorescently labeled strand G was subsequently annealed with strand H to produce the ds-DNA sample used in the anisotropy experiments.

All samples were studied in 10 mM TRIS buffer (pH 7.4). Annealing was performed by heating the two strands to 90 °C and cooling down slowly to avoid formation of secondary structures. The fluorescence intensities of Cy3 and Cy5 did not change after annealing, indicating that both dyes are chemically stable at the temperatures used in the process.

Steady-State Fluorescence. Fluorescence spectra were measured using a QuantaMaster-4/2005SE spectrofluorometer (PTI,

NJ). Temperature was controlled with a water circulation bath and measured inside the cuvette with a calibrated thermocouple. Fluorescence quantum yields were measured relative to the corresponding value for carboxytetramethylrhodamine in methanol ($\phi = 0.68$).[14] Excitation spectra were obtained by scanning the excitation wavelength while keeping the emission wavelength fixed at 700 nm. A built-in quantum counter was used to correct excitation spectra for the wavelength-dependent lamp output and possible temporal instabilities. Emission spectra were acquired by scanning the emission wavelength while keeping the excitation wavelength fixed at 510 nm. The output of a standardized lamp was used to correct emission spectra from wavelength-dependent variations in detector sensitivity and transmission of optical components.

Time-Resolved Fluorescence. Time-resolved fluorescence intensity decays were measured using time correlated single-photon counting (TCSPC) at room temperature, as described elsewhere.[10] The sample was excited with vertically polarized light while the emission polarizer was kept at the magic angle with respect to the excitation polarizer for the intensity decays and at vertical and horizontal positions for the anisotropy decays. The instrument response function (IRF) was measured using a 2% Ludox scattering solution (Sigma Aldrich, MO). The measured fwhm of the IRF was typically about 40 ps. Intensity decays were obtained from the measured decays by iterative deconvolution, assuming that the intensity decay function can be represented by a sum of exponentials. The goodness of the fit was evaluated from the χ^2 value and the randomness of the residuals.

Time-resolved fluorescence anisotropy decays were calculated from the experimentally measured decays without deconvolution as $r(t) = (I_V - I_H \times G)/(I_V + 2I_H \times G)$, where the subscript refers to the position of the emission polarizer (vertical or horizontal). The G-factor accounting for differences in system response for the two polarized emission components was determined by the tail matching method using a solution of free rhodamine 6G in methanol, for which the rotational correlation time is much faster than the fluorescence lifetime.

Determination of FRET Efficiencies. FRET efficiencies for each sample were measured by at least two independent methods.

(a) Steady-State Excitation Spectra. In this method, the corrected excitation spectrum of the sample containing the FRET pair is fitted to the following equation:

$$I(\lambda_{exc}) = K\,[\varepsilon^{D}(\lambda_{exc})E_{FRET} + \varepsilon^{A}(\lambda_{exc})] \tag{3}$$

where E_{FRET} represents the FRET efficiency, K is a constant, and $\varepsilon^{D,A}$ represents the wavelength-dependent extinction coefficients of the donor and acceptor, respectively. The shapes of the functions $\varepsilon^{D}(\lambda_{exc})$ and $\varepsilon^{A}(\lambda_{exc})$ were obtained by measuring the excitation spectra of dsDNA samples containing *i*Cy3 or *i*Cy5 only. The peaks of these functions were fixed at 150,000 M^{-1} cm^{-1} (Cy3) and 250,000 M^{-1} cm^{-1} (Cy5), which are the accepted extinction coefficients of these dyes at their absorption maxima.

We prefer this method over methods that utilize a donor-only reference to calculate the FRET efficiency from the decrease in donor intensity due to several reasons. First, the determination from the excitation spectrum does not require a donor-only reference. Second, it does not require the knowledge of the absorbance of the sample. Low absorbances are hard to determine precisely when microcuvettes are needed due to limited amounts of sample.

Note that the presence of a donor-only sample (molecules with donor but not acceptor) does not affect the outcome of the FRET measurement by this method. Thus, for samples 2 and 3, we performed these measurements in the presence of a 10% excess Cy3-strand to ensure complete annealing. FRET measurements for sample 1, which contains both the donor and acceptor in the same strand, were performed with a large excess of unlabeled complementary strand to ensure the absence of doubly labeled ssDNA.

(b) Time-Resolved Intensity Decay of Cy3. FRET efficiencies were obtained from time-resolved data as described in ref 4.

Briefly, the intensity decay of Cy3 was fitted to a sum of exponential terms

$$I_{Cy3}(t) = \sum_i \alpha_i \exp(-t/\tau_i) \tag{4}$$

and FRET efficiencies were calculated from the average decay time of the donor in the absence (τ_D^0) and the presence (τ_D) of acceptor as follows:

$$E = 1 - \frac{\langle \tau_D \rangle}{\langle \tau_D^{\,0} \rangle} \tag{5}$$

where

$$\langle \tau_D \rangle = \frac{\sum_i \alpha_i \tau_i}{\sum_i \alpha_i} \tag{6}$$

In this case, samples 2 and 3 were prepared with a 10% excess of the acceptor-labeled strand to ensure that all donor molecules were part of helical DNA. Excess of acceptor-labeled ssDNA does not interfere with this method.

(c) Single-Molecule Spectroscopy. The FRET efficiency of sample 1 was also measured at the single-molecule level to ensure that the large value measured in bulk was not an artifact due to the presence of a secondary structure in which the donor and acceptor are much closer than what is predicted for B-DNA (see Results and Discussion). Measurements were done in a single-molecule confocal setup assembled in house. Briefly, a 532 CW laser (Crystalaser, Reno, NV) was attenuated to approximately 100 μW and focused into a 1.4 NA objective lens (Olympus PlanApo 100X/1.4NA Oil). Fluorescence was collected with the same objective, passed through a pinhole to reject out-of-focus light, and split into a donor and an acceptor signal with a dichroic mirror (Omega XF2021). Donor and acceptor intensities were measured with 1 ms resolution using two independent avalanche photodiodes (Perkin-Elmer Optoelectronics, SPCM-AQR14). Band pass filters were used in front of each detector to further reduce unwanted light (Omega 3RD560-620 for the donor and Chroma BP670/40 for the acceptor). Experiments were performed in the presence of 140 mM β-mercaptoethanol to reduce Cy5 blinking.

FRET efficiencies were calculated after correcting for contributions from the background (~1.5 counts/ms for the donor and 3 counts/ms for the acceptor) and contributions from crosstalk (5% of the Cy3 intensity detected in the acceptor detector). The signal was also corrected for differences in detector efficiency and fluorescence quantum yield as:

$$E = \frac{I_A}{I_A + \gamma I_D} \quad (7)$$

where γ was calculated from the measured intensities of sample 3 using the bulk FRET efficiency reported in Figure 2.

A threshold of (I_A or I_D) > 14/ms was used to minimize the contributions of background and other unwanted signals to the FRET calculation.

Results

Time-resolved fluorescence anisotropy provides a straightforward way of observing rotational motion in the nanosecond time scale. In this technique, the sample is excited with linearly polarized light, which selectively excites molecules with transition dipole moments aligned parallel to the polarization plane of the excitation source. The polarization plane of the emitted light depends on the orientation of the molecule at the moment of emission, so it becomes increasingly random as the fluorophore rotates. The extent of randomization is measured by the anisotropy ($r(t)$, see Materials and Methods) and decreases in a time scale determined by the time scales of rotation of the fluorescent probe.[4] A value of $r = 0$ indicates complete randomization, corresponding to a situation where the dye emits from all orientations with equal probability. Figure 3 shows the anisotropy decays of Cy3 free in solution (blue), attached to dsDNA through a six-carbon flexible linker (red), and incorporated into the backbone of DNA (black). The decay of the free dye is monoexponential with a rotational correlation time $\tau_r = 380$ ps (reported in previous work, see ref 10).

It is evident from these results that the dye does not rotate freely in the nanosecond time scale when a flexible linker is used for covalent attachment. Only 36% of the decay is dictated by fast local motions ($\tau_r = 0.21 \pm 0.08$ ns) while the rest of the decay corresponds to a 23 ± 6 ns rotational correlation time, which is characteristic of the overall tumbling motion of dsDNA.[15] In contrast, local motion is practically suppressed in the sample containing the backbone modification (Figure 3, black trace). In this case, only 15% of the decay is dictated by fast motions (0.8 ± 0.6 ns), while the rest decays with a 26 ± 4 ns rotational correlation time similar to the previous case. The anisotropy decay obtained with the *i*Cy5-dsDNA sample is identical within experimental error to the one measured with *i*Cy3, and it is not shown for clarity.

For the backbone modifications, the orientation of the transition dipole moments of the two fluorophores is controlled by the architecture of the double strand. To illustrate this, we measured the FRET efficiency of three ds-DNA samples containing a *i*Cy3-*i*Cy5 pair at different positions. Sample 1 was prepared by annealing the following sequence with a nonlabeled complementary strand: $(N)_{15}$-*iCy3*-$(N)_{29}$-*iCy5*-$(N)_{14}$ (here, N represents a DNA base, see Materials and Methods for the exact sequences). Samples 2 and 3 were prepared by annealing an oligo containing *i*Cy3 with the complementary strand containing *i*Cy5 in the position opposite to the nucleotide marked in bold face: $(N)_{15}$-*iCy3*-$(N)_{26}$-**A**-$(N)_{17}$ (sample 2) and $(N)_{18}$-*iCy3*-$(N)_{23}$-**A**-$(N)_{17}$ (sample 3). FRET efficiencies were measured by at least two independent methods, and R_{DA} values were taken as the distance between the middle carbon atoms in the polymethine chains of the Cy3 and Cy5 molecules. Models were constructed in HyperChem (Gainesville, FL) using a standard B-DNA structure. An error of ±3 Å was estimated from the geometrical model based on the flexibility of the single C−C bonds in the linkers joining the Cy dyes and the DNA phosphates. The structure of Figure 1C should be regarded only as a cartoon to aid in the interpretation of the results, and it is not intended to represent the actual position of the different atoms in the equilibrated system. Such a calculation is beyond the scope of this work.

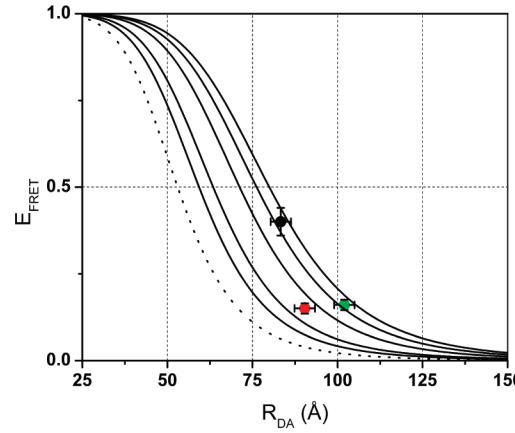

Figure 2. Lines: predicted FRET efficiencies (E_{FRET}) for $R_0 = 53$ Å (dotted line) and R_0 calculated for this particular sample (solid lines) assuming $\kappa^2 = {}^2/_3$ (left), 1, 2, 3, and 4 (right). The symbols represent the experimentally measured FRET efficiencies for sample 1 (green), sample 2 (red), and sample 3 (black). The uncertainty in the FRET efficiency is estimated as ~10%. Donor−acceptor distances were estimated from a B-DNA model as described in the text.

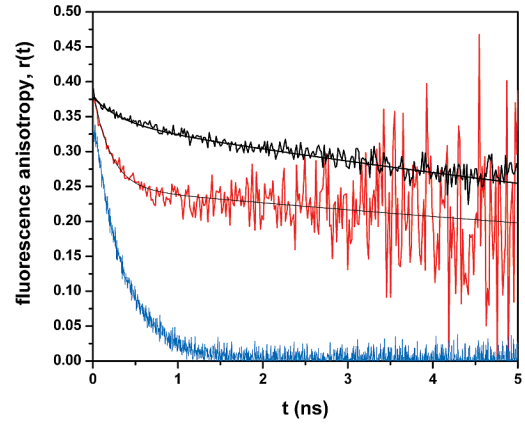

Figure 3. Time-resolved fluorescence anisotropy of free Cy3 (blue), Cy3 attached to dsDNA through a six-carbon flexible linker (red), and the backbone internal modification studied in this work (black). The decay of the free dye is monoexponential with a rotational correlation time $\tau_r = 380$ ps. The decays on DNA were fitted to a biexponential equation (see text).

The lowest electronic transition in carbocyanine dyes is polarized along the principal axis of the molecule,[16] so we expect the two oscillating dipoles to be approximately collinear when the two dyes are on the same strand and separated by a number of base pairs equal to a multiple of ten (the number of bases per helical turn in B-DNA). In fact, we observe that the FRET efficiency of sample 1, where the Cy3 and Cy5 dyes are on the same strand and separated by 102 Å (three helical turns), is 0.16, consistent with a κ^2 value of approximately 3.2. This value is close to the theoretical limit of four, which is predicted for the case in which the two dipole moments are collinear. The lines in Figure 2 represent the predicted E_{FRET} vs R_{DA} behavior for different values of R_0 according to eq 1. The dotted line corresponds to a value of $R_0 = 53$ Å, which is a widely used value for the Cy3-Cy5 pair.[17] However, it is important to stress that this value depends on the fluorescence quantum yield of Cy3 (eq 2), which has been shown to depend strongly on the

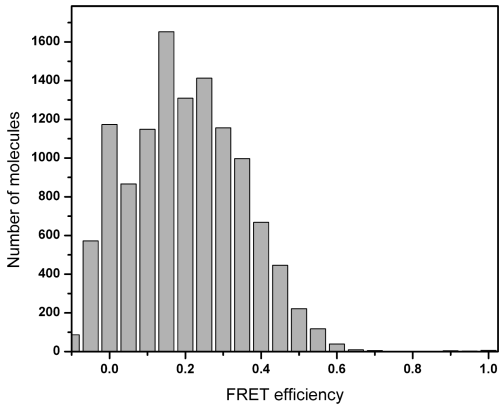

Figure 4. Single-molecule FRET efficiency of sample 1 showing the absence of subpopulations with large E_{FRET} values.

environment in which the dye is located.[10] In this work, we measured $\phi_D^0 = 0.31 \pm 0.02$ for the Cy3 backbone modifications on dsDNA at room temperature. Using this value and the calculated overlap integral in eq 2, we obtain $R_0 = 63.4(\kappa^2)^{1/6}$. The solid lines in Figure 2 represent the behavior expected for $\kappa^2 = {}^2/_3$, 1, 2, 3, and 4, according to this equation. It is evident that no FRET would be detected at $R_{DA} = 102$ Å if it were not for the favorable orientation factor.

This is further demonstrated by the results of the measurement with sample 2, in which the dyes are separated by 90 Å. It is interesting to observe that this sample presents virtually the same FRET efficiency as sample 1, while R_{DA} is 12 Å shorter in this case. This is a clear demonstration of the importance of the κ^2 factor in the measurement of distances from FRET measurements. A further decrease in the distance by 7 Å (sample 3) brings the dipoles to a favorable orientation again, and the FRET efficiency increases to a value compatible with $\kappa^2 \sim 3.5$. In this case, the dyes are located on opposite strands with a separation $R_{DA} = 83$ Å (approximately 2.5 helical turns). The unusually large FRET efficiency at this distance is a consequence of the near-parallel alignment of the dipoles. Note that the common assumption of $R_0 = 53$ Å would yield $R_{DA} = 56$ Å, almost a helical turn of DNA shorter than the distance estimated from the B-DNA structure.

Sample 1 contains both the donor and acceptor in the same strand, so it is possible in principle to imagine that the high FRET efficiencies measured in this work are a consequence of secondary structures in which the DNA strand loops on itself, bringing the donor and the acceptor close together. Secondary structures were predicted using the "mfold" server.[18] The program predicted the existence of a variety of secondary structures with melting temperatures in the 30−40 °C range. To address this possibility, we performed single-molecule experiments at room temperature and bulk FRET experiments as a function of temperature. The FRET efficiency in bulk decreased steadily from $E_{FRET} = 0.16$ at 23 °C to $E_{FRET} = 0.10$ at 63 °C, but these changes can be quantitatively accounted for considering the variations in R_0 due to changes in the donor quantum yield with temperature (ϕ_D^0(63 °C)/ϕ_D^0(23 °C) = 2.4). Once this correction is taken into account, the difference between the values of R_{DA} measured at these two temperatures is less than 5%, well within the error of the determination. This suggests that there are no contributions from secondary structures in our measurements. The results of the single-molecule FRET experiment (Figure 4) further support this conclusion. We observe a peak around $E_{FRET} = 0$, typical of single-molecule experiments where acceptor photobleaching plays an important role,[19] and a population around $E_{FRET} = 0.2$, which we assign to sample 1. The most important aspect of this result, however, is the absence of molecules with a high FRET efficiency, which would indicate the presence of a subpopulation of molecules with low R_{DA} values. It is important to stress that the width of the distribution does not necessarily indicate the existence of a distribution of donor−acceptor distances. The primary source of broadening in single-molecule measurements is often shot noise due to the low photon count numbers that are measured in these experiments, which creates a distribution of FRET efficiencies even when a sample with a single R_{DA} value is measured.

Discussion

The orientation factor is the most widely discussed source of uncertainties in FRET measurements, which led to a widespread use of flexible linkers with the purpose of maximizing the rotational freedom of the dye when attached covalently to DNA. However, time-resolved fluorescence anisotropy decays show that the mobility of the dye is partially restricted in the time scale relevant for fluorescence. The longer rotational correlation time present in the fluorescence anisotropy decay (23 ± 6 ns) is consistent with the expected tumbling time of dsDNA of this size and similar to values reported by Ramreddy et al. using the fluorescent nucleotide analog 2-aminopurine.[15] The fact that 64% of the anisotropy decay of Cy3 follows the overall tumbling of DNA suggests that a fraction of the Cy3 molecules are strongly interacting with the double helix, proving that flexible linkers do not provide the expected rotational freedom that would be needed to safely assume a $\kappa^2 = {}^2/_3$ value. In contrast, backbone modifications remain mostly rigid in the nanosecond time scale, so the relative orientation between the donor and acceptor transition dipole moments is not expected to change in the time scale relevant for FRET. In addition, this rigidity decreases the efficiency of the nonradiative pathways that compete with fluorescence, including photoisomerization from the first excited state, and as a consequence the fluorescence quantum efficiency of both dyes increases with respect to the values measured when flexible linkers are used instead. It is important to keep in mind that R_0 values depend on the fluorescence quantum efficiency of the donor (eq 2), so these values need to be measured for the particular type of biochemical modification used to attach the dye to the DNA.

The idea of using rigidly attached fluorophores to control dye orientation in FRET measurements has been also explored by Lewis et al.[20] and Iqbal et al.,[21] who used fluorophores positioned at the ends of the double helix to use the helical scaffold as a template to control orientation. In both cases, the fluorophores are stacked on the ends of the helix, so their relative orientation depends on the length of the stretch of DNA. Lewis et al. used stilbene dicarboxamide as the donor, which can be synthetically attached to both DNA strands, reducing the rotational freedom of the dye on the DNA. However, a drawback of this approach is that stilbene dicarboxamide absorbs in the UV and it is not suitable for most biophysical applications, which require dyes with very high photostabilities and absorption wavelengths far from the spectral regions where sample autofluorescence and Raman scattering limit the ability to detect small concentrations of fluorescently labeled DNA. Iqbal et al. took advantage of the fact that Cy3 and Cy5 are predominantly stacked onto the ends of the helix,[22,23] and observed a modulation of FRET efficiency with helix length caused by changes in the relative orientation of the dipoles. Yet, results show that this modulation is less than that calculated for a fully rigid attachment of the

fluorophores, which is consistent with our previous fluorescence anisotropy reports that show some flexibility of Cy3 when bound to the end of DNA.[10] In addition, this approach is limited to short strands of DNA, since it requires that both Cy3 and Cy5 are placed at the ends of the double helix. In contrast, the backbone modifications studied in this work are commercially available from DNA vendors such as Integrated DNA Technologies (Coralville, IA) and are incorporated at any desired location during solid-state synthesis. An added advantage of incorporating fluorescent modifications during solid-state synthesis is that this procedure minimizes the amount of donor-only or acceptor-only sample, which is a major problem when fluorophores are reacted with amino-modified nucleotides post-synthesis. If the dye is not incorporated during solid state synthesis, the resulting oligonucleotide will be shorter and thus easily removed by electrophoresis or HPLC. In contrast, nonlabeled amino-modified oligonucleotides have the same length as the fluorescently labeled strands and are much harder to purify.

In conclusion, we have observed surprisingly high FRET efficiencies for sample 1, in which the donor and acceptor are on the same strand and separated by three helical turns. We believe this result is a consequence of the favorable orientation of the two dipoles, imposed by the helical geometry of the DNA. The same FRET efficiency was measured for a sample in which the dyes are 12 Å closer (sample 2), demonstrating the importance of orientation in FRET measurements. Furthermore, the restricted mobility of the dye is advantageous to minimize other sources of uncertainty in FRET experiments, such as photophysical effects that may arise from environmental heterogeneity, and variations in donor−acceptor caused by the flexible linkers used for covalent attachment.

Acknowledgment. This work was supported by an NSF CAREER grant to M.L (PHY-0644414).

References and Notes

(1) Stryer, L.; Haugland, R. P. *Proc. Natl, Acad. Sci. U.S.A.* **1967**, *58*, 719.
(2) Klostermeier, D.; Millar, D. P. *Methods* **2001**, *23*, 240.
(3) Lilley, D. M. J.; Wilson, T. J. *Curr. Opin. Chem. Biol.* **2000**, *4*, 507.
(4) Valeur, B. *Molecular Fluorescence: Principles and Applications*; Wiley-VCH: Weinheim, Germany, 2001.
(5) Dale, R. E.; Eisinger, J.; Blumberg, W. E. *Biophys. J.* **1979**, *26*, 161.
(6) Dosremedios, C. G.; Moens, P. D. J. *J. Struct. Biol.* **1995**, *115*, 175.
(7) van der Meer, B. W. *Rev. Mol. Biotechnol.* **2002**, *82*, 181.
(8) VanBeek, D. B.; Zwier, M. C.; Shorb, J. M.; Krueger, B. P. *Biophys. J.* **2007**, *92*, 4168.
(9) Joo, C.; Balci, H.; Ishitsuka, Y.; Buranachai, C.; Ha, T. *Annu. Rev. Biochem.* **2008**, *77*, 51.
(10) Sanborn, M. E.; Connolly, B. K.; Gurunathan, K.; Levitus, M. *J. Phys. Chem. B* **2007**, *111*, 11064.
(11) Dolghih, E.; Roitberg, A. E.; Krause, J. L. *J. Photochem. Photobiol., A* **2007**, *190*, 321.
(12) Unruh, J. R.; Gokulrangan, G.; Lushington, G. H.; Johnson, C. K.; Wilson, G. S. *Biophys. J.* **2005**, *88*, 3455.
(13) Vamosi, G.; Gohlke, C.; Clegg, R. M. *Biophys. J.* **1996**, *71*, 972.
(14) Magde, D.; Brannon, J. H.; Cremers, T. L.; Olmsted, J. *J. Phys. Chem.* **1979**, *83*, 696.
(15) Ramreddy, T.; Rao, B. J.; Krishnamoorthy, G. *J. Phys. Chem. B* **2007**, *111*, 5757.
(16) Levitus, M.; Negri, R. M.; Aramendia, P. F. *J. Phys. Chem.* **1995**, *99*, 14231.
(17) Ishii, Y.; Yoshida, T.; Funatsu, T.; Wazawa, T.; Yanagida, T. *Chem. Phys.* **1999**, *247*, 163.
(18) Zuker, M. *Nucleic Acids Res.* **2003**, *31*, 3406.
(19) Deniz, A. A.; Dahan, M.; Grunwell, J. R.; Ha, T. J.; Faulhaber, A. E.; Chemla, D. S.; Weiss, S.; Schultz, P. G. *Proc. Natl. Acad. Sci. U.S.A.* **1999**, *96*, 3670.
(20) Lewis, F. D.; Zhang, L. G.; Zuo, X. B. *J. Am. Chem. Soc.* **2005**, *127*, 10002.
(21) Iqbal, A.; Arslan, S.; Okumus, B.; Wilson, T. J.; Giraud, G.; Norman, D. G.; Ha, T.; Lilley, D. M. J. *Proc. Natl. Acad. Sci. U.S.A.* **2008**, *105*, 11176.
(22) Iqbal, A.; Wang, L.; Thompson, K. C.; Lilley, D. M. J.; Norman, D. G. *Biochemistry* **2008**, *47*, 7857.
(23) Norman, D. G.; Grainger, R. J.; Uhrin, D.; Lilley, D. M. J. *Biochemistry* **2000**, *39*, 6317.

JP810842U